ACOUSTIC CHARACTERIZATION OF BONDED OAK-APPLE PANELS BY NORMAL-INCIDENCE MEASUREMENTS AND INVERSE EQUIVALENT-FLUID MODELING

Rui Ribeiro[1], Isabel Cardoso[1], Tiago Brilhante[1], Pedro Pinto[1], Artur Ferreira[2], Nuno Gama[2], Vânia Teixeira[3]

[1]*Amplitude Acoustics – Acústica e Vibração, Lda. – Maia, Portugal*

[2]*CICECO—Aveiro Institute of Materials and University of Aveiro, Aveiro, Portugal*

[3]*Lightenjin II – Indústria de Iluminação, Lda. – Águeda, Portugal*

Abstract

The search for sustainable alternatives to conventional porous absorbers has increased interest in bio-based materials for acoustic applications. This paper investigates the normal-incidence sound absorption performance of bonded oak-apple panels manufactured using two different processing strategies and compares their behavior with that of a commercial polyurethane foam (PUF) of equal thickness. Measurements were carried out using an in-situ acoustic impedance method based on combined sound pressure and particle velocity sensing. To support the interpretation of the experimental results, an equivalent-fluid modeling approach based on the Johnson-Champoux-Allard (JCA) formulation was adopted. An inverse parameter identification procedure was implemented to estimate effective macroscopic properties from the measured absorption spectra, including airflow resistivity, porosity, tortuosity, and equivalent viscous and thermal characteristic-length factors. The identified parameters are discussed as effective descriptors of a heterogeneous bio-based porous composite rather than intrinsic material constants. The results show that oak-apple panels provide competitive mid and high frequency absorption and confirm the potential of this naturally derived material for sustainable acoustic treatment solutions.

Keywords: *bio-based absorber, oak galls, sound absorption, equivalent-fluid model, inverse characterization*

Corresponding author: *rui.ribeiro@amplitude-ac.eu*

1. Introduction

Sound-absorbing materials play an important role in building acoustics, industrial noise control, and environmental noise mitigation. Their relevance has grown in parallel with increasing awareness of the adverse effects of long-term noise exposure and with the demand for acoustically comfortable indoor environments [1]. At the same time, the construction sector is under growing pressure to adopt more sustainable material solutions, driven by environmental regulation, green-building frameworks, and the need to reduce embodied impacts.

Conventional porous absorbers such as mineral wool, fiberglass, and PUF remain widely used because they offer a favorable balance between acoustic efficiency, especially at mid and high frequencies, cost, ease of application, and even their fire reaction properties. All of the above characteristics are extremely relevant and support the vast applicability of these products, however, they also present well-known limitations related to recyclability, embodied energy, mechanical fragility, and, in some cases, handling and health concerns [2]. These limitations have encouraged the search for alternative sound-absorbing materials with lower environmental impact and competitive acoustic performance. Within this context, bio-based materials have received considerable attention. It has been demonstrated that the sound absorption potential of porous materials derived from natural fibers and agricultural by-products, including coconut coir, hemp, olive leaves, and other forms of biomass waste [3]-[6]. Beyond their acoustical behavior, such materials may contribute to circular-economy strategies by valorizing low-value raw resources and supporting local supplier chains.

The present work builds upon earlier investigations into the acoustic behavior of oak apples, or oak galls [7]. These are naturally occurring hypertrophic formations that develop on oak species as a result of insect-induced biochemical interactions [8]. Their internal structure is lightweight, porous, and highly irregular, with interconnected air cavities that suggest acoustical behavior analogous to that of conventional porous absorbers. Previous exploratory measurements indicated that bonded oak-apple panels can achieve absorption levels comparable to, and in some frequency regions, higher than those of commercial PU foams of similar thickness [7].
Although the absorption coefficient provides a direct measure of acoustic performance, it does not by itself reveal the physical mechanisms responsible for sound dissipation. For this reason, equivalent-fluid models have become valuable tools in the characterization of porous absorbers. Models such as JCA describe the acoustic response of porous media through a reduced set of effective macroscopic parameters. Those can be related to pore geometry, flow resistance, and thermo-viscous losses [9], [10]. When combined with inverse fitting procedures, these models make it possible to estimate effective frequency dependent descriptors directly from acoustic measurements, helping manufacturers and researchers in the development of optimized materials and solutions [11].
This paper presents an experimental and model-based characterization of bonded oak-apple panels. Normal-incidence absorption was measured using an in-situ impedance method, and an inverse JCA fitting procedure was used to identify effective macroscopic parameters from the measured data. This approach aims to provide a deeper physical interpretation of the observed acoustic performance and to further assess the potential of oak apples as a sustainable material for acoustic treatment applications

2. Materials

Oak apples, also referred to as oak galls, are naturally occurring growths that develop on several oak species as a result of interactions between the host tree and gall-inducing insects [8]. They typically present a near-spherical geometry with diameters on the order of 20 to 40 mm and consist of an outer shell enclosing a lightweight internal tissue. Although their morphology varies with species and growth conditions, the internal structure generally exhibits a porous and cellular organization with interconnected cavities.
From an acoustical perspective, this morphology suggests behavior similar to that of open-cell porous absorbers, in which sound attenuation is governed by viscous and thermal losses within a connected pore network [9], [10]. To qualitatively examine these features, representative oak-apple specimens were observed by optical microscopy and scanning electron microscopy (SEM). The SEM images indicate an irregular open cellular structure spanning multiple length scales, which supports the use of equivalent-fluid modeling as a first-order representation of the material.

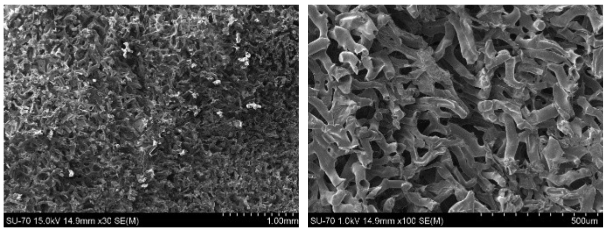

Figure 1. Scanning electron microscopy (SEM) - oak apple internal cellular structure, showing an open and irregular porous morphology

For the experimental campaign, two bonded oak-apple panel specimens were manufactured from randomly sourced oak apples. In both cases, a polysiloxane-based adhesive was used as binding agent because of its mechanical stability and limited penetration into the porous tissue. Before bonding, the oak apples were cut open so that the internal porous structure was exposed at the panel surface, thereby increasing the interaction between the incident sound field and the pore network. The two specimens differed mainly in the level of mechanical processing. In Sample A, the oak apples were cut into halves and assembled with limited additional machining, thus preserving much of the natural geometry of each element, including the rigid outer layer of the galls. In Sample B, the material was further trimmed and sanded into approximately cuboid pieces composed predominantly of the internal porous tissue. This second approach produced a more regular surface and tighter packing. Both panels had nominal dimensions of 200 mm x 200 mm, an approximate thickness of 30 mm. Both bulk densities are close to 110 kg/m^3, despite tighter packing for Sample B.

Figure 2. Bonded oak-apple panel specimens: Sample A (left), assembled from halved oak apples, and Sample B (right), assembled from machined cuboid elements

The use of two processing strategies allows a qualitative assessment of how machining and packing affect the effective acoustic response. While the intrinsic porosity of the oak-apple tissue is expected to remain broadly similar, the mesostructure introduced by bonding, void distribution, and surface regularity may significantly affect the measured sound absorption behavior as well as the effective flow resistivity and tortuosity inferred from inverse modeling, as discussed in subsequent sections.
A first observation of both samples indicates that Sample B is likely to present a more homogeneous behavior, governed by thermal and viscous phenomena, whilst Sample A's geometric properties should result in more prominent scattering and resonant effects.

3. Methodology

3.1 Measurement approach

The sound absorption performance of the oak-apple panels was evaluated for a normally incident sound field using an in-situ acoustic impedance measurement method based on combined sound pressure and particle velocity (PU) sensing. This approach enables the estimation of surface impedance and reflection coefficient without requiring large samples or impedance-tube testing and is therefore well suited to exploratory studies of novel materials [11].
Measurements were performed using a *Microflown* in-situ impedance setup consisting of a compact spherical loudspeaker mounted on a mechanically decoupled frame, together with a PU probe positioned at a fixed distance from the source. *Microflown Velo* software was used for data-acquisition and operating.

Figure 3. In-situ impedance measurement setup

The measurements were conducted in an unoccupied office room with a floor area of approximately 30 m^2, bare plastered walls, a wooden laminated floor on a concrete slab, and acoustic ceiling tiles.
The adopted method and procedure relied on previous studies to optimize and inform on how to perform measurements with the PU probe technique regarding sample size, methodology, and probe location [11].

3.2 Determination of the normal-incidence absorption coefficient

The normal-incidence sound absorption coefficient, α_n, was derived from the complex reflection coefficient R under the assumption of negligible sound transmission through the specimen. It is defined as:

$$\alpha_n = 1 - | R |^2 \quad (1)$$

The measurement system estimates the reflection coefficient from the measured specific acoustic surface impedance. For a locally reacting surface under normal incidence, the reflection coefficient may be written as

$$R = \frac{\frac{Z_m}{Z_{ff}} - 1}{\frac{Z_m}{Z_{ff}}\left(\frac{d}{d+2h}\right)\left(\frac{e^{jk(d+2h)}}{e^{jkd}}\right) + 1}\left(\frac{d+2h}{d}\right) e^{2jkh} \quad (2)$$

where Z_m is the measured surface impedance and Z_{ff} is the characteristic impedance of air. This formulation assumes locally reacting behavior and plane-wave incidence at the sample surface. As discussed in previous studies, deviations from these assumptions become more significant at lower frequencies because of wavefront curvature, probe-positioning uncertainty, and room-related effects [12].

3.3 Frequency range and data processing

In view of the practical limitations associated with compact in-situ impedance measurements, the analysis was restricted to the 500 Hz to 10 kHz range. Below this interval, the confidence in the estimated surface impedance and derived absorption coefficient decreases significantly, especially for relatively small samples and non-anechoic environments. To improve robustness and to facilitate comparison with reference materials, the measured absorption coefficients were presented in third-octave bands.
For benchmarking purposes, a commercial open-cell PUF sample with a nominal density of 30 kg/m^3 and the same nominal dimensions as the oak-apple panels was measured using the same setup and procedure. This ensured consistency in the measurement conditions and enabled a direct comparison, performance wise, with a widely used conventional porous absorber.

4. Experimental Results

The measured normal-incidence sound absorption coefficients of the two oak-apple panel specimens are presented in Fig. 4, in third-octave bands over the frequency range from 500 Hz to 10 kHz. For reference, the absorption coefficient of the commercial open-cell PUF of identical thickness, measured under the same conditions, is also shown.

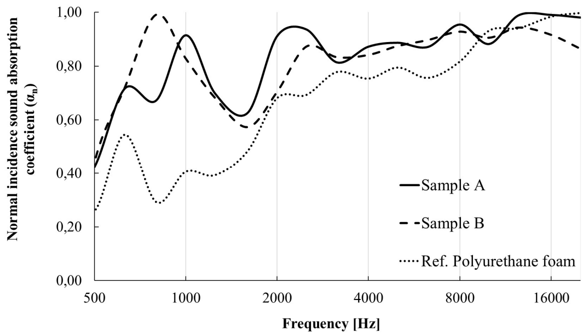

Figure 4. Oak-apple panels (Samples A and B) and 30 kg/m^3 polyurethane foam normal-incidence sound absorption coefficients (1/3-octave-band)

Both oak-apple specimens exhibited high sound absorption over a broad frequency range, with absorption coefficients approaching or exceeding 0.8 above, approximately, 1 kHz. In the mid-frequency range, between 500 Hz and 1600 Hz, Samples A and B show substantially higher absorption than the reference PUF, with peak differences observed around the 1 kHz. At higher frequencies, the absorption performance of all materials tends to converge, although the oak-apple maintain slightly higher values across the spectrum.
The two oak-apple samples also showed similar overall trends but differed in the smoothness and local variability of their spectra. Sample B, which underwent additional machining and presented a more

homogeneous surface topology, displayed a smoother frequency response at mid and high frequencies.
Sample A, by contrast, showed more pronounced band-to-band fluctuations, particularly below 4000 Hz.
While Sample B is built with a single layer of gall elements, with approximately the same thickness, Sample A consists of the superposition of two out-of-phase half-gall layers, which may explain the differences in absorption peaks in the 1000 Hz region and the more evident resonance effect observed around 2000 Hz. Therefore, it is plausible to relate the different behaviors to the differences in surface regularity, local cavity distribution, and inter-element void geometry within each bonded panel.

5. Equivalent-Fluid Modeling and Inverse Parameter Identification

5.1 Modeling framework

To support a physically informed interpretation of the experimental results, the acoustic behavior of the oak-apple panels was analyzed using an equivalent-fluid modeling approach. In this framework, the porous material is represented as a rigid-frame porous medium saturated with air, and its acoustic response is described by a frequency-dependent effective density and effective bulk modulus. Among the available equivalent-fluid models, the JCA formulation was adopted because of its widespread use for porous cellular and fibrous media [9], [10]. In the implemented formulation, the model response is defined by the airflow resistivity σ, layer thickness d, open porosity ϕ, tortuosity α_∞, and two shape factors controlling the equivalent viscous and thermal characteristic lengths, Λ and Λ'. The viscous and thermal lengths were written

$$\Lambda = \frac{1}{s}\sqrt{\frac{8\eta\alpha_\infty}{\phi\sigma}} \tag{3}$$

$$\Lambda' = \frac{1}{s'}\sqrt{\frac{8\eta\alpha_\infty}{\phi\sigma}} \tag{4}$$

where η is the dynamic viscosity of air, and s and s' are dimensionless fitting factors. This parametrization reduces the number of independent geometric descriptors while retaining enough flexibility to adapt the model to the measured spectra. Using the standard JCA expressions, the effective density ρ_e and effective bulk modulus K_e were computed as frequency-dependent complex quantities [9], [10]. The characteristic impedance Z_c and wave number k of the equivalent fluid were then obtained from:

$$Z_c = \sqrt{\rho_e K_e} \tag{5}$$

$$k = \omega\sqrt{\frac{\rho_e}{K_e}} \tag{6}$$

For a porous layer backed by a rigid termination, the surface impedance Z_s is given by

$$Z_s = \frac{Z_c}{tanh(jkd)} \tag{7}$$

and the normal-incidence absorption coefficient follows from Eqs. (1) and (2).

5.2 Inverse identification procedure

The effective porous parameters were estimated by inverse fitting of the measured normal-incidence absorption spectra. The optimization was performed over the frequency range from 500 Hz to 10 kHz using a differential-evolution algorithm, which provides a robust global-search strategy for non-convex parameter-estimation problems.
Six parameters were treated as unknowns:

i) airflow resistivity (σ),
ii) layer thickness, open porosity (ϕ),
iii) tortuosity (α_∞),
iv) dimensionless fitting factors (s and s') controlling the equivalent viscous and thermal characteristic lengths.

The optimization was carried out within physically admissible bounds selected to ensure numerical stability and consistency with the expected behavior of lightweight porous materials.
The objective function combined a weighted mean-squared error between measured and modeled absorption with a smoothness penalty applied to the high-frequency part of the predicted spectrum. A larger weight was assigned to the 750 Hz to 1100 Hz interval in order to prioritize the fit in the region containing the main experimental absorption peak and resonance-like behavior. In addition, the sum of the absolute first differences of the modeled absorption above 3 kHz was included as a regularization term to discourage non-physical oscillations and overfitting of measurement noise.
This inverse procedure should be interpreted as an effective macroscopic characterization rather than a direct measurement of intrinsic porous parameters. The adopted weighting and regularization improve robustness and spectral consistency, but they also introduce a degree of model bias toward the most relevant spectral features of the measured response. Moreover, part of the residual mismatch may be related not only to measurement uncertainty but also to intrinsic characteristics of the specimens, including the geometric arrangement of the bonded gall elements.

5.3 Identified effective parameters

The resulting effective JCA parameters for Samples A and B are summarized in Table 1. The identified values fall within ranges commonly reported for conventional porous absorbers and bio-based materials, supporting the validity of the modeling approach.
The characteristic lengths reported in the table were derived from the fitted parameters (JCA).

Table 1. Effective JCA parameters for the oak-apple panel specimens vrs literature reference values for PUF

Parameter	SampA	Samp B	Ref. values
Airflow resistivity σ [Pa.s/m^2]	58126	28414	1000 - 100000 [13]
Open porosity ϕ	0.95	0.96	0.95 - 0.99 [14]

Tortuosity, α_∞	2.45	3.44	1.0 - 2.3 [13], [14]
Viscous length Λ [μm]	59.3	56.7	50 – 200 [13], [14]
Thermal length Λ' [μm]	67.4	58.4	100 – 400 [13], [14]

The resulting parameters exhibit substantial coherence with the ranges typically associated with acoustic-graded PUF. This alignment confirms that the bonded assemblies behave fundamentally as rigid-frame porous absorbers. However, significant deviations are observed in tortuosity and thermal characteristic length. The high tortuosity values, indicate that Samples A and B present a more complex internal cellular morphology than a typical PUF, whilst the observation that the thermal length is approximately equal to the viscous length points to a more uniform pore geometry.
The inverse fitting results indicate comparable open porosity for both panels, with values close to 0.95, suggesting that the overall accessible pore volume is broadly similar in the two configurations. The main differences are observed in the transport-related parameters, where "Sample":

i) "A" exhibits a higher effective airflow resistivity,
ii) "B" shows lower resistivity but higher tortuosity and slightly shorter characteristic lengths.

These differences indicate that the processing route influenced the effective acoustic transport behavior of the bonded assembly. Possibly, for Sample B the additional machining altered its mesoscale arrangement (gall elements) and the connectivity of the exposed pore network, thereby changing the balance between flow resistance and effective propagation path complexity. These parameters should be interpreted as effective descriptors derived from inverse modeling rather than direct measurements of the underlying pore geometry.

5.4 Model validation

The agreement between measured and modeled absorption coefficients is illustrated in Fig. 5. In both cases, the JCA model reproduces the main spectral trend, particularly the overall high absorption above 1 kHz and the local maxima observed in the mid-frequency range. The agreement is moderate rather than exact, which is consistent with the heterogeneous character of the bonded panels and the simplifying assumptions of the equivalent-fluid approach.

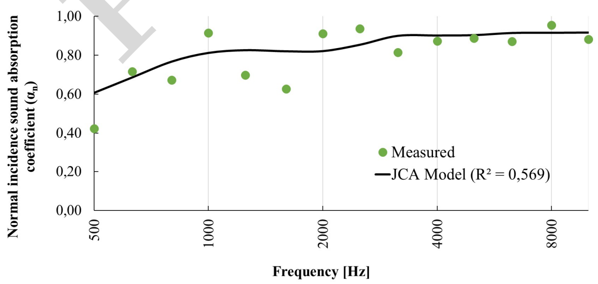

(a)

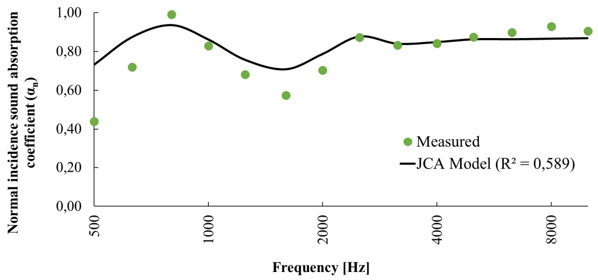

(b)

Figure 5. Comparison between measured and JCA-modeled normal-incidence absorption coefficients for Sample A, (a), and Sample B, (b)

For Sample A, the fitted model yields $R^2 = 0.569$ and reproduces the gradual increase in absorption towards high frequencies, although it smooths part of the local variability observed in the measured data. For Sample B, the agreement is slightly improved, with $R^2 = 0.589$, and the model captures the more structured mid-frequency behavior while still underrepresenting some local fluctuations. These results confirm that the model provides a meaningful effective description of the specimens, while also indicating that part of the measured response is governed by structural heterogeneity not explicitly resolved by the JCA model.

5.5 Limitations and scope of applicability

It is important to emphasize that the identified parameters represent effective macroscopic properties derived from inverse modeling rather than intrinsic material constants. The heterogeneous nature of the bonded oak-apple panels, combined with the assumptions inherent to equivalent-fluid models, imposes limitations on the physical interpretation of individual parameters. Nevertheless, the adopted approach provides a consistent and pragmatic framework for linking experimental absorption data with model-based descriptors and for positioning oak-apple panels within the broader landscape of porous sound-absorbing materials.

6. Discussion

The experimental and model-based results together indicate that bonded oak-apple panels behave acoustically as efficient porous absorbers over the investigated frequency range. The high absorption values observed above approximately 1 kHz can be reasonably attributed to the open and interconnected cellular structure of the oak-apple tissue, which promotes viscous and thermal dissipation in the pore network. Cumulative, the bonded-panel architecture introduces a second level of structural organization that likely affects the effective flow paths and may contribute to local resonant or scattering effects.
The comparison between Samples A and B suggests that processing and packing configuration influence the effective acoustic behavior in a measurable way. Panels assembled from more regularly machined elements tend to show smoother absorption spectra and are expected to yield more spatially uniform effective parameters. By

contrast, panels preserving a greater fraction of the natural geometry may exhibit stronger local variability because of the irregular distribution of inter-element cavities and surface roughness. These effects are not explicitly represented in the JCA formulation and are therefore absorbed into the fitted effective parameters.

The inverse identification procedure is useful precisely because it provides a compact description of this complex behavior. Even when the global fit is not perfect, the extracted parameters offer a meaningful way to compare different processing strategies and to relate the oak-apple panels to conventional porous absorbers. However, the fitted quantities should be interpreted with caution as they provide the acoustic response of the complete bonded assembly, under the specific test configuration, rather than the intrinsic material constants of the oak-apple tissue alone.

From an application perspective, the results are encouraging. Compared with a conventional PUF, used as a reference of equal thickness, the oak-apple panels provide comparable or superior absorption in the mid-frequency range while relying on a naturally derived raw material. This suggests that oak apples may constitute a promising candidate for sustainable acoustic treatments, particularly where moderate thickness, lightweight construction, and bio-based content are valued.

Further work should include direct measurements of open porosity and airflow resistivity, additional inverse fits for other panel assemblies. Complementary testing and validation would be beneficial, including studies at lower frequencies. Other performance indicators such aging, fire behavior, mechanical durability and manufacturing repeatability would be valuable.

7. Conclusions

This paper investigated bonded oak-apple panels as a sustainable bio-based alternative to conventional porous sound absorbers. Measuring normal-incidence showed that 30 mm thick oak-apple panels can provide high and broadband sound absorption, being comparable to, and in some frequency regions better than, that of a commercial PUF of equal thickness.

The comparison between the two panel configurations highlighted the role of material processing and structural organization in shaping the effective acoustic response. Panels assembled from more uniformly machined elements tended to exhibit smoother spectra, indicating that mesostructural regularity influences the effective flow paths taken by the incident sound field.

An inverse equivalent-fluid characterization based on the JCA model was used to estimate effective macroscopic porous parameters from the measured absorption data. The fitted values were found to be physically plausible and consistent with the behavior expected from lightweight porous absorbers. At the same time, the moderate fit quality obtained for the available case confirms that these parameters should be regarded as effective descriptors of a heterogeneous bonded composite rather than intrinsic material constants.

Overall, the results support the potential of oak apples as a viable bio-based material for acoustic treatment applications. Their competitive absorption performance, combined with the possibility of model-based parameterization, provides a useful basis for further material optimization and for future comparisons with other sustainable absorbers.

References

[1] F. Aletta and J. Kang, "Promoting healthy and supportive acoustic environments: Going beyond the quietness," *Int. J. Environ. Res. Public Health*, vol. 16, no. 24, p. 4988, 2019.

[2] D. Oldham, C. Egan, and G. Cookson, "Sustainable acoustic absorbers from the biomass," *Appl. Acoust.*, vol. 72, no. 6, pp. 350-363, 2011.

[3] R. Zulkifli, M. Zulkarnain, and J. Mohd Nor, "Noise control using coconut coir fiber sound absorber with porous layer backing and perforated panel," *Amer. J. Appl. Sci.*, vol. 7, no. 2, pp. 260-264, 2010.

[4] D. Zhang, X. Zhou, Y. Gao, and L. Lyu, "Structural characteristics and sound absorption properties of waste hemp fiber," *Coatings*, vol. 12, no. 12, p. 1907, 2022.

[5] I. M. Belda et al., "Evaluacion acustica de paneles fabricados con hojas de olivo aglomerados con matriz polimerica," *in Proc. Tecniacustica 2023*, Cuenca, Spain, 2023.

[6] R. Thomazelli, F. Caetano, and S. Bertoli, "Acoustic properties of green walls: Absorption and insulation," *in Proc. Meetings Acoust.*, vol. 28, Art. no. 015002, 2017.

[7] R. Ribeiro et al., "Sound absorption coefficient analysis of bonded oak apple panels," *in Proc. Tecniacustica 2024*, Faro, Portugal, 2024.

[8] M. Schonrogge, G. Stone, and J. Crawley, "The biology and ecology of oak galls," *Biol. Rev.*, vol. 75, no. 4, pp. 593-629, 2000.

[9] D. L. Johnson, J. Koplik, and R. Dashen, "Theory of dynamic permeability and tortuosity in fluid-saturated porous media," *J. Fluid Mech.*, vol. 176, pp. 379-402, 1987.

[10] Y. Champoux and J.-F. Allard, "Dynamic tortuosity and bulk modulus in air-saturated porous media," *J. Appl. Phys.*, vol. 70, no. 4, pp. 1975-1979, 1991.

[11] M. Ribera et al., "In-situ acoustic characterization of porous materials using a PU-Probe," *in Proc. Tecniacustica 2023*, Cuenca, Spain, 2023.

[12] B. B. Hosseini, M. Hornikx, and J. Yang, "In situ acoustic characterization of locally reacting porous materials by means of PU measurement and model fitting," *Appl. Acoust.*, vol. 191, p. 108664, 2022.